Supporting Information

Supplementary Methods:

Animal Ethics and Sinoatrial Node Dissociation

This study was carried out in accordance with the US Animal Welfare Act and the National Research Council's *Guide for the Care and Use of Laboratory Animals* and was conducted according to a protocol that was approved by the University of Colorado-Anschutz Medical Campus Institutional Animal Care and Use Committee.

Six- to eight-week old male C57BL/6J mice were obtained from Jackson Laboratories (Cat. #000664). Animals were anesthetized by isofluorane inhalation and euthanized under anesthesia by cervical dislocation. Hearts were excised and bathed in warmed (35ºC) modified Tyrode's solution (in mM: 140 NaCl, 5.4 KCl, 1.2 KH_2PO_4, 5 HEPES, 5.55 glucose, 1 $MgCl_2$, 1.8 $CaCl_2$; pH adjusted to 7.4 with NaOH) containing 10 U/mL heparin. The ventricles were removed and the sinoatrial node was dissected from the atrial tissue, as defined by the borders of the crista terminalis, the interatrial septum, and the superior and inferior vena cavae.

The sinoatrial node was cut into three to five strips, which were digested at 35ºC for in a low Ca^{2+} modified Tyrode's solution (in mM: 140 NaCl, 5.4 KCl, 1.2 KH_2PO_4, 5 HEPES, 18.5 glucose, 0.066 $CaCl_2$, 50 taurine, 1 mg/ml BSA; pH adjusted to 6.9 with NaOH) containing either 4.75 U elastase (Worthington Biochemical) and 3.75 mg Liberase TM (Roche) for 10-12 minutes or 1064 U type II collagenase (Worthington), 9 U elastase (Worthington), and 652 μg type XIV protease (Sigma) for 30 min. Following enzymatic digestion, SAMs were dissociated by mechanical trituration with a fire-polished glass pipette (~2 mm diameter) for 5 - 8 min at 35ºC in a modified KB solution (in mM: 100 K^+-glutamate, 10 K^+-aspartate, 25 KCl, 10 KH_2PO_4, 2 $MgSO_4$, 20 taurine, 5 creatine, 0.5 EGTA, 20 glucose, 5 HEPES, and 0.1% BSA; pH

adjusted to 7.2 with KOH). Ca^{2+} and BSA were gradually introduced to the cell suspension in 5 steps over the course of 22 min to a final concentration of 1.8 mM Ca. Cells were stored in KB solution at room temperature for up to 10 hours before electrophysiological recordings.

Electrophysiology

Data were acquired at 5-20 kHz and low-pass filtered at 1 kHz using an Axopatch 1D or 200B amplifier, Digidata 1322a or 1440a A/D converter, and ClampEx software (Molecular Devices). Bath and perfusing solutions were maintained at 35ºC for all recordings with a feedback-controlled temperature controller (TC-344B, Warner Instruments). Reported data have been corrected for calculated liquid junction potentials using the calculator in ClampEx software. Fast (pipette) capacitance was compensated in all voltage-clamp recordings. Recording pipettes were pulled from borosilicate glass (VWR International) using a Sutter Instruments P-97 horizontal puller. Pipette resistances ranged from 1.5 to 5 MΩ.

Sinoatrial Myocyte Current Clamp Recordings

An aliquot (~50 μl) of the isolated SAM suspension was transferred to a glass bottomed recording chamber and cells were allowed to settle for ~5 minutes before perfusion with extracellular solution. Recording Tyrode's solution (in mM: 140 NaCl, 5.4 KCl, 5 HEPES, 5 Glucose, 1 $MgCl_2$, 1.8 $CaCl_2$; pH adjusted to 7.4 with NaOH) containing 1 nM isoproterenol was used to record AP firing rates. Pipettes were filled with an internal solution composed of (in mM): 110 K-aspartate, 20 KCl, 1 $MgCl_2$, 5 EGTA, 5 Mg-ATP, 5 creatine phosphate, and 5 HEPES; pH adjusted to 7.2 with KOH. After a gigaohm seal and whole-cell configuration were established, cells were lifted off the bottom of the recording chamber and the amplifier was set to

current clamp mode with zero injected current. 30 s of stable AP firing was recorded followed by up to 2.5 min of AP firing with perfusion of 30 μM ivabradine in Tyrode's solution.

Sinoatrial Myocyte Square-Wave Voltage-Clamp Recordings

Whole-cell Ca^{2+} currents were recorded in a K^+ current-blocking extracellular solution (in mM: 130 tetraethylammonium chloride, 2 $CaCl_2$, 1 $MgCl_2$, 10 4- aminopyridine, and 10 HEPES; pH adjusted to 7.4 with CsOH) with a pipette solution consisting of 130 mM CsCl, 1 mM $MgCl_2$, 10 mM Hepes, 10 mM EGTA, 4 mM Mg-ATP, and 0.1 mM NaGTP, with the pH adjusted to 7.2 with CsOH. Total Ca^{2+} current was measured in response to depolarizing steps between -50 to +40 mV from a holding potential of -90 mV. L-type Ca^{2+} currents were measured in response to depolarizing steps between -50 to +40 mV from a holding potential of -60 mV where T-type current is inactivated. T-type currents were estimated by subtracting the L-type Ca^{2+} current from total Ca^{2+} in each cell. Ivabradine and isradipine block of currents were assessed following perfusion of 30 μM ivabradine or 3 μM isradipine as indicated. Leak subtraction was performed using a P/4 protocol.

Whole-cell K^+ currents were measured in response to depolarizing steps between -40 to +50 mV from a holding potential of -50 mV in recording Tyrode's extracellular solution containing 1 nM isoproterenol and 3 μM isradipine to block voltage-gated Ca^{2+} currents. Intracellular solution consisted of 135 mM KCl, 1 mM $MgCl_2$, 4 mM Mg-ATP, 0.1 mM Na-GTP, 5 mM EGTA, 5 mM HEPES, and 6.6 mM Na-phosphocreatine, with the pH adjusted to 7.2 with KOH. Steady-state current was measured at the end of the depolarizing step, while the transient current was measured by subtracting steady-state current from the peak outward current during a depolarizing step. Inhibition by ivabradine and the K-blocker cocktail were assessed

following perfusion of 30 μM ivabradine and/or 10 mM TEA, 1 mM barium, and 1 μM E4031 as indicated.

Whole-cell I_f recordings were measured in recording Tyrode's solution containing either 1 nM or 1 μM isoproterenol as indicated. Pipettes were filled with K-aspartate intracellular solution containing (in mM): 140 K-aspartate, 13.5 mM NaCl, 1.8 $MgCl_2$, 0.1 EGTA, 4 Mg-ATP, 0.3 GTP (tris salt), 14 creatine phosphate, and 9 HEPES, pH 7.2 with KOH. I_f was measured as the time-dependent current elicited by 3 s steps to potentials between -60 and -150 mV from a holding potential of -50 mV. Inhibition by ivabradine, isradipine, and the K-blocker cocktail were assessed following perfusion of 30 μM ivabradine, 3 μM isradipine, and/or 10 mM TEA, 1 mM barium, and 1 μM E4031 as indicated. Activation voltage-dependence was determined by calculating conductance from time-dependent inward currents as $G=I/V-V_{rev}$, where G is conductance, I is current, V is the step potential, and V_{rev} is the I_f reversal potential (-30 mV; (1). The normalized conductance for each cell was fit with a single Boltzmann equation to calculate the midpoint and slope of the relationship. Time constants and the relative amplitudes of the fast and slow components of I_f activation and deactivation were measured by double-exponential fits. Deactivation was measured during 3 s steps to potentials between -50 and +50 mV following a 1 s step to -150 mV.

Sinoatrial Myocyte AP Clamp Recordings

For AP-clamp recordings, SAMs were constantly perfused at 35ºC with recording Tyrode's extracellular solution containing 1 nM or 1 μM isoproterenol as indicated. Spontaneous APs were first recorded in the whole-cell current clamp configuration and then 10 s of the AP recording were included in the command voltage protocol in voltage-clamp experiments to

isolate the specific currents flowing during the AP (Fig. S2). The protocol was first used to record ionic currents in the absence of compensation for cellular capacitance to ensure that the amplifier currents were near zero (2). To isolate I_f, we subtracted currents immediately before and after applying 30 μM ivabradine, while in the constant presence of 1 mM $BaCl_2$, 10 mM TEA, 1 μM E-4031, 30 μM TTX and 3 μM isradipine. I_f block was monitored during hyperpolarizing steps to -90 mV or -120 mV. Cells were held at -40 mV between sweeps, with a total inter-pulse interval of 20 s between the start of each sweep. AP-elicited I_f was averaged from 4 consecutive APs during the final 2 s of each sweep to allow currents to reach their steady-state for the given AP-waveform.

To account for incomplete block of I_f by ivabradine, the subtracted currents during AP-clamp were scaled for the measured fractional block achieved in the hyperpolarizing pulses from the same cell. In some cells, the current inhibited by ivabradine included a component of potassium current that remained in the blocker cocktail, as evidenced by an outward current evoked by a step to 0 mV from a holding potential of -40 mV (where I_f is deactivated) or by reversal potentials of the ivabradine-sensitive current that were substantially negative to the reversal potential for I_f under the same ionic conditions (~31 mV, Fig. 3D, Fig. S3B). Analysis was restricted to cells in which no potassium current contamination was evident in the ivabradine-sensitive current.

HEK Cell Electrophysiology

HEK 293 cells stably expressing HCN4 (generously provided by Martin Biel's laboratory, Ludwig-Maximilians Universität, Munich, Germany) were grown at 37ºC at 5% CO_2 in high glucose DMEM with L-glutamine, supplemented with 10% FBS, 100 U/mL penicillin,

and 100 μg/ml streptomycin (all from Thermo Fisher Scientific, Waltham, MA). To maintain the HEK-HCN4 stable line, the media was further supplemented with 200 μg/mL Hygromycin B (Invivogen, San Diego, CA). HEK 293 cells were negative for mycoplasma infection. Testing for mycoplasma infection was performed at the Molecular Biology Core Facility in the Barbara Center for Childhood Diabetes at the University of Colorado Anschutz Medical Campus. 24 hours prior to experiments cells were seeded on protamine-coated glass coverslips. Recordings were performed in recording Tyrode's extracellular solution with 1-2 MΩ borosilicate glass pipettes filled with K-Aspartate intracellular solution (same formulation as sinoatrial I_f recordings) containing 0 or 1 mM cAMP as indicated. All recordings were performed 35ºC. For 0 mM and 1 mM cAMP recordings, murine sinoatrial APs previously recorded at 1 nM isoproterenol or 1 μM isoproterenol were used as voltage commands, respectively. HCN4 currents were recorded by subtracting currents immediately before and after applying 30 μM ivabradine, while in the presence of a "CK" blocker cocktail containing: 1 mM $BaCl_2$, 10 mM TEA, 3 μM E-4031, and 3 μM isradipine. HCN4 current amplitude and current-voltage relationships were calculated from an average of 3 consecutive APs from each cell.

Modelling

We modified an existing Hodgkin-Huxley type model of I_f in murine SAMs (3) and manually tuned the parameters to fit our experimental datasets obtained in SAMs in the presence of 1 nM or 1 μM isoproterenol. Values of parameters used are reported in Table S6. In 1 nM and 1 μM isoproterenol I_f models, the total I_f current is calculated as the sum of the inward sodium ($I_{f,Na}$) and the outward potassium ($I_{f,K}$) components scaled by the relative ion permeabilities through the channel pore (Equation 1):

1) $$I_f = I_{f,Na} + I_{f,K}$$

The two individual components were calculated as follows (Equations 2-4):

2) $$I_{f,K} = pK * G_f * P_O * (Vm - E_K)$$

3) $$I_{f,Na} = (1 - pK) * G_f * P_O * (Vm - E_{Na})$$

4) $$pK = \frac{Eq - E_{Na}}{E_K - E_{Na}}$$

Where Vm is the membrane potential, G_f is the maximal I_f conductance, P_o is the channel open probability, pK is the permeability to potassium relative to sodium, E_q is the I_f equilibrium potential, and E_{Na} and E_K are the Nernst potentials of Na^+ and K^+, respectively. In our novel formulation, the activation/deactivation gate n determining P_O is controlled by both fast and slow processes n_f and n_s (Equations 5-6).

5) $$P_O = n = (n_f * \frac{1}{n_{Ratio}+1}) + (n_s * \frac{n_{Ratio}}{n_{Ratio}+1})$$

6) $$n_{Ratio} = \frac{a}{e^{-b*(Vm+c)} + e^{b*(Vm+d)}}$$

Where n_{Ratio} indicates the distribution of channels between slow and fast gating modes n_s and n_f at a given membrane potential, and was obtained fitting the ratio between the amplitudes of the slow and fast components estimated from biexponential fitting of current traces (Fig. S5). Changes over time in n_f and n_s are calculated as follows (Equations 7-11):

7) $$\frac{dn_i}{dt} = \frac{n_\infty - n_i}{\tau_i}$$

8) $$n_\infty = \frac{1}{1 + e^{(Vm - V_{1/2})/z}}$$

9) $$\tau_i = \frac{\tau_{i0}}{\propto_i + \beta_i}$$

10) $$\propto_i = e^{-k_i * (Vm + \propto_{i,1/2})}$$

11) $$\beta_i = e^{k_i * (Vm + \beta_{i,1/2})}$$

Where n_∞ is the steady-state activation common to both n_f and n_s (Fig. S5D), and τ_i is the time constant of activation or deactivation at a given voltage for either the fast (Fig. S5F) or slow (Fig. S5G) component of the activation gate. α_i and β_i are the activation and deactivation rates for either the fast or slow component of the activation gate. Values of parameters used in Equations 1-11 are reported in Table S6.

To model I_f during the sinoatrial AP, sets of AP waveform recordings from the 1 nM and 1 μM isoproterenol AP-clamp experiments were used to stimulate the 1 nM and 1 μM isoproterenol models, respectively. Current-voltage relationships were calculated from the average of 3 consecutive APs. Model conductances were scaled such that the current amplitude at either -90 mV or -120 mV was the same as that experimentally recorded in the SAM from which the voltage protocol was derived. The model of HCN2 gating uses the equations from the non-cAMP bound state of the model proposed by Wang *et al.* (4). The HCN1 model uses the gating scheme proposed by Battefeld *et al.* (5). Single-state Hodgkin-Huxley type models were chosen for HCN1 and HCN2 to be consistent with our models of I_f. The maximal conductances of the HCN1 and HCN2 models were scaled such that the maximal inward currents during AP clamp simulations were similar to the 1 nM I_f model to facilitate comparisons of altered gating. All models were simulated in the Spyder Python environment using a forward Euler method with a 200 μs time step.

Supplementary Table 1: Off-target effects of ivabradine in SAMs

	Control Peak Density (pA/pF)	3 µM Ivabradine Peak Density (pA/pF)	30 µM Ivabradine Peak Density (pA/pF)
I_f	-22.86 ± 3.84 (7)	-13.23 ± 3.33 (7) P = 0.0157 vs. Control	-1.01 ± 0.37 (7) P < 0.0001 vs. Control
I_{Ca}	-11.36 ± 1.29 (5)	N/A	-7.50 ± 0.61 (5) P = 0.0236 vs. Control
$I_{Ca,L}$	-10.01 ± 1.06 (5)	N/A	-5.70 ± 0.81 (5) P = 0.0046 vs. Control
$I_{Ca,T}$	-1.35 ± 0.29 (5)	N/A	-1.80 ± 0.74 (5) P = 0.6329 vs. Control
$I_{K,Trans}$	-9.57 ± 1.50 (5)	N/A	-5.21 ± 1.65 (5) P = 0.0391 vs. Control
$I_{K,SS}$	2.78 ± 0.22 (5)	N/A	1.89 ± 0.19 (5) P = 0.0191 vs. Control

I_f: Funny Current; I_{Ca}: Total Ca^{2+} current; $I_{Ca,L}$: L-type Ca^{2+} current; $I_{Ca,T}$: T-type Ca^{2+} current; $I_{K,Trans}$: Transient K^+ current; $I_{K,SS}$: Steady-state K^+ current.

Peak Ca^{2+}, K^+, and I_f currents were measured at 0 mV, +40 mV, and -130 mV, respectively. Data are averages ± SEM with number of replicates in parentheses. Tests for statistical differences in peak I_f density were performed using repeated measures ANOVAs of currents recorded with either 3 µM or 30 µM ivabradine matched to currents recorded in control conditions (1 mM $BaCl_2$) in the same cell. Tests for statistical differences in peak current density of Ca^{2+} and K^+ currents were performed using paired t-tests of currents recorded with 30 µM ivabradine matched to currents recorded in control conditions in the same cell.

Supplementary Table 2: Ca^{2+} and K^+ blocker effects in SAMs

	Control Peak Density (pA/pF)	Ca^{2+} and/or K^+ Blockers Peak Density (pA/pF)	Ca^{2+} and/or K^+ Blockers with 30 µM Ivabradine Peak Density (pA/pF)
I_{Ca}	-8.22 ± 1.70 (9)	-0.96 ± 0.16 (9) P = 0.0022 vs. Control	N/A
$I_{Ca,L}$	-6.86 ± 1.59 (9)	-0.57 ± 0.09 (9) P = 0.0030 vs. Control	N/A
$I_{Ca,T}$	-5.08 ± 0.91 (9)	-0.46 ± 0.06 (9) P = 0.00057 vs. Control	N/A
$I_{K,Trans}$	6.78 ± 0.87 (9)	1.25 ± 0.27 (9) P < 0.0001 vs. Control	0.81 ± 0.24 (9) P = 0.7173 vs. Blockers
$I_{K,SS}$	3.90 ± 0.26 (9)	2.63 ± 0.24 (9) P < 0.0001 vs. Control	2.41 ± 0.26 (9) P = 0.3127 vs. Blockers
I_f	-17.25 ± 4.60 (8)	-15.76 ± 4.32 (8) P = 0.8726 vs. Control	-0.73 ± 0.34 (8) P = 0.0002 vs. Control

I_{Ca}: Total Ca^{2+} current; $I_{Ca,L}$: L-type Ca^{2+} current; $I_{Ca,T}$: T-type Ca^{2+} current; $I_{K,Trans}$: Transient K^+ current; $I_{K,SS}$: Steady-state K^+ current; I_f: Funny Current.

Peak Ca^{2+}, K^+, and I_f currents were measured at 0 mV, +40 mV, and -130 mV, respectively. Data are averages ± SEM with number of replicates in parentheses. Tests for statistical differences in peak current density of Ca^{2+} currents were performed using paired t-tests of currents recorded with isradipine matched to currents recorded in control conditions in the same cell. Tests for statistical differences in peak current density of K^+ currents were performed using repeated measures ANOVAs of currents recorded with a K^+ blocker cocktail in the absence or presence of ivabradine matched to currents recorded in control conditions in the same cell. Tests for statistical differences in peak I_f density were performed using repeated measures ANOVAs of

currents recorded with the NCK blocker cocktail in the absence or presence of ivabradine matched to currents recorded in control conditions (1 mM $BaCl_2$) in the same cell.

Supplementary Table 3: Ivabradine-sensitive current during AP clamp in SAMs

	1 nM Isoproterenol	1 μM Isoproterenol	1 μM vs. 1 nM
Firing Rate (bpm)	268 ± 212 (10)	340 ± 26 (10)	P = 0.0474
Cellular Capacitance (pF)	33.7 ± 2.6 (10)	30.1 ± 2.54 (10)	P = 0.3336
Inward Current			
Peak Current - (pA)	-17.7 ± 2.9 (10)	-26.7 ± 4.4 (10)	P = 0.1046
Peak Current Density - (pA/pF)	-0.54 ± 0.09 (10)	-0.90 ± 0.12 (10)	P = 0.0240
Charge Movement (pC)	-1.61 ± 0.35 (10)	-2.64 ± 0.64 (10)	P = 0.1713
Charge Density - (pC/pF)	-0.045 ± 0.009 (10)	-0.085 ± 0.014 (10)	P = 0.0283
Rate of Charge Movement (pC/s)	-6.40 ± 1.19 (10)	-13.54 ± 2.38 (10)	P = 0.0150
Conductance - (nS)	0.25 ± 0.05 (10)	0.57 ± 0.09 (10)	P = 0.0058
Outward Current			
Peak Current - (pA)	29.1 ± 5.2 (10)	36.9 ± 6.5 (10)	P = 0.3597
Peak Current Density - (pA/pF)	0.93 ± 0.17 (10)	1.26 ± 0.22 (10)	P = 0.2584
Charge movement (pC)	0.35 ± 0.08 (10)	0.56 ± 0.17 (10)	P = 0.2692
Charge Density - (pC/pF)	0.011 ± 0.003 (10)	0.018 ± 0.005 (10)	P = 0.2658
Rate of Charge Movement (pC/s)	1.64 ± 0.45 (10)	2.96 ± 0.79 (10)	P = 0.1648
Conductance - (nS)	0.49 ± 0.07 (10)	0.56 ± 0.11 (10)	P = 0.6027
Corrected Outward Current			
Peak Current - (pA)	10.5 ± 2.6 (10)	17.9 ± 5.0 (10)	P = 0.2064
Peak Current Density - (pA/pF)	0.34 ± 0.09 (10)	0.62 ± 0.18 (10)	P = 0.1895
Charge movement (pC)	0.19 ± 0.05 (10)	0.29 ± 0.11 (10)	P = 0.3890
Charge Density - (pC/pF)	0.006 ± 0.002 (10)	0.009 ± 0.003 (10)	P = 0.3497
Rate of Charge Movement (pC/s)	0.86 ± 0.25 (10)	1.51 ± 0.50 (10)	P = 0.2604
Conductance - (nS)	0.15 ± 0.05 (10)	0.27 ± 0.07 (10)	P = 0.2200
Reversal Potential (mV)	-31.3 ± 2.2 (10)	-28.2 ± 1.8 (10)	P = 0.2769
-60 mV Current			

Upstroke - (pA)	-8.6 ± 2.5 (10)	-17.8 ± 2.7 (10)	
Downstroke - (pA)	-9.3 ± 2.3 (10)	-16.5 ± 3.6 (10)	
	P = 0.6826	P = 0.2982	

All data are averages ± SEM with number of replicates in parentheses. Corrected outward currents are calculated from extrapolated linear fits to data from potentials more negative than -20 mV to eliminate contamination by unblocked K^+ currents in some cells. Tests for statistical differences between 1 nM and 1 μM isoproterenol were performed using unpaired t-tests. Tests for statistical differences between current at -60 mV between the upstroke and downstroke of the action potential were performed using paired t-tests.

Supplementary Table 4: Ivabradine-sensitive current in response to AP Clamp in HCN4-expressing HEK cells

	0 mM cAMP	1 mM cAMP	0 mM vs. 1 mM
Inward Current			
Peak Current - (pA)	-62.7 ± 14.3 (7)	-264.1 ± 54.9 (7)	P = 0.0040
Peak Current Density - (pA/pF)	-2.05 ± 0.71 (7)	-5.23 ± 1.07 (7)	P = 0.0136
Charge movement (pC)	-5.51 ± 1.33 (7)	-23.54 ± 4.91 (7)	P = 0.0041
Charge Density - (pC/pF)	-0.195 ± 0.078 (7)	-0.466 ± 0.095 (7)	P = 0.0474
Conductance - (nS)	1.75 ± 0.42 (7)	7.07 ± 1.45 (7)	P = 0.0046
Outward Current			
Peak Current - (pA)	26.6 ± 9.6 (7)	135.6 ± 38.1 (7)	P = 0.0169
Density - (pA/pF)	0.71 ± 0.16 (7)	2.58 ± 0.65 (7)	P = 0.0160
Charge movement (pC)	0.31 ± 0.13 (7)	1.02 ± 0.29 (7)	P = 0.0489
Charge Density - (pC/pF)	0.007 ± 0.002 (7)	0.019 ± 0.005 (7)	P = 0.0482
Conductance - (nS)	0.75 ± 0.23 (7)	5.11 ± 1.05 (6)	P = 0.0011
Reversal Potential (mV)	-21.2 ± 4.8 (7)	-22.9 ± 3.0 (7)	P = 0.7590
-60 mV Current			
Upstroke - (pA)	-42.0 ± 11.4 (7)	-209.7 ± 43.2 (7)	
Downstroke - (pA)	-34.6 ± 8.3 (7)	-200.8 ± 43.5 (7)	
	P = 0.2594	P = 0.0011	

All data are averages ± SEM with number of replicates in parentheses. Tests for statistical differences between 0 mM and 1 mM cAMP were performed using unpaired t-tests. Tests for statistical differences between current at -60 mV between the upstroke and downstroke of the action potential were performed using paired t-tests.

Supplementary Table 5: Simulated funny current in response to AP waveforms

	1 nM Isoproterenol	1 μM Isoproterenol
Inward Current		
Peak - (pA)	-7.5 ± 2.7 (10)	-15.9 ± 2.3 (10)
Charge - (pC)	-1.23 ± 0.38 (10)	-4.36 ± 0.80 (10)
Outward Current		
Peak - (pA)	18.9 ± 5.9 (10)	33.6 ± 4.2 (10)
Charge - (pC)	0.26 ± 0.07 (10)	0.85 ± 0.16 (10)
-60 mV Current		
Upstroke - (pA)	-7.1 ± 1.9 (10)	-29.1 ± 3.6 (10)
Downstroke - (pA)	-5.9 ± 1.6 (10)	-23.6 ± 2.7 (10)

All data are averages ± SEM with number of replicates in parentheses.

Supplementary Table 6: Modelling parameters for equations 1-11

	1 nM Isoproterenol model	1 μM Isoproterenol model	Units
G_f	11.79		nS
E_q	-35.4		mV
E_{Na}	70.49		mV
E_K	-86.96		mV
$V_{1/2}$	103.18	88.53	mV
z	11.6	9.15	
τ_{f0}	0.7	0.035	ms
k_f	0.025	0.04	mV^{-1}
$\alpha_{f,1/2}$	340	330	mV
$\beta_{f,1/2}$	-160	-170	mV
τ_{s0}	70	10	ms
k_s	0.015	0.025	mV^{-1}
$\alpha_{s,1/2}$	300	285	mV
$\beta_{s,1/2}$	-200	-215	mV
a	0.015	0.003	
b	0.025	0.03	
c	300	330	mV
d	-200	-170	mV

Where E_{Na} and E_K were calculated using the Nernst equations with 140 mM extracellular Na^+, 10 mM intracellular Na^+, 5.4 mM extracellular K^+, and 140 mM intracellular K^+.

Supplementary Figure 1:

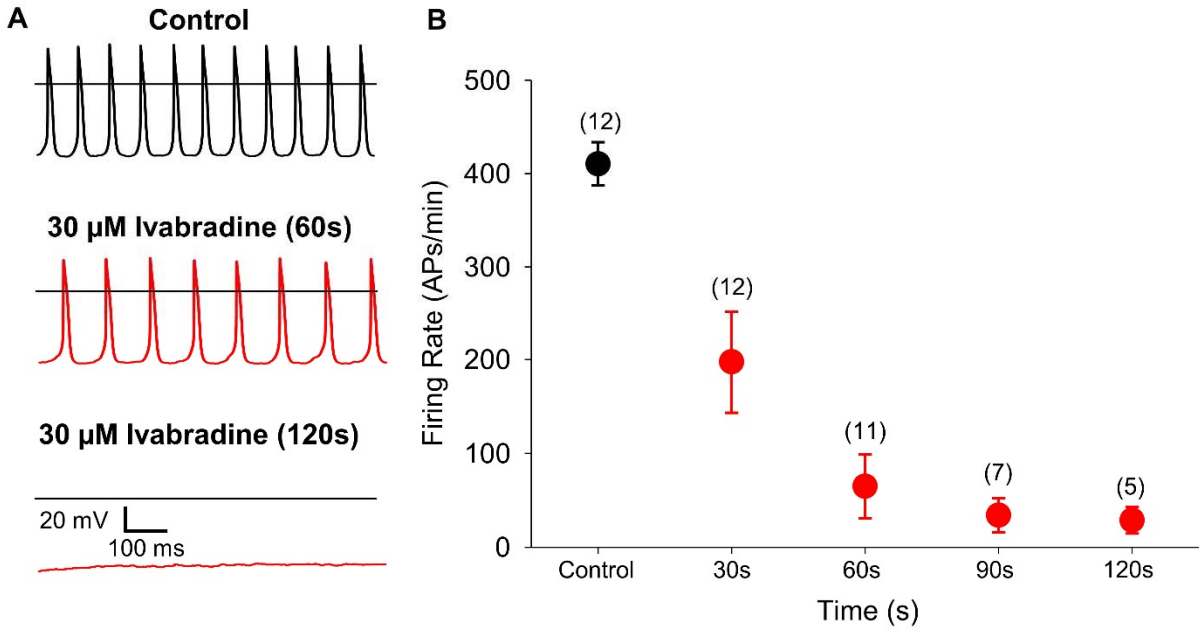

Figure S1: Ivabradine slows AP firing in SAMs

A: Representative APs recorded from a sinoatrial myocyte in control Tyrode's solution containing 1 nM isoproterenol (*top*) or following 60 s (*middle*) or 120 s (*bottom*) of perfusion with 30 µM ivabradine. Horizontal lines indicate 0 mV. **B:** Average AP firing rates (± SEM) before (*black*) or at different time points during 30 µM ivabradine perfusion (*red*). Number of observations for each time point are given in parentheses.

Supplementary Figure 2:

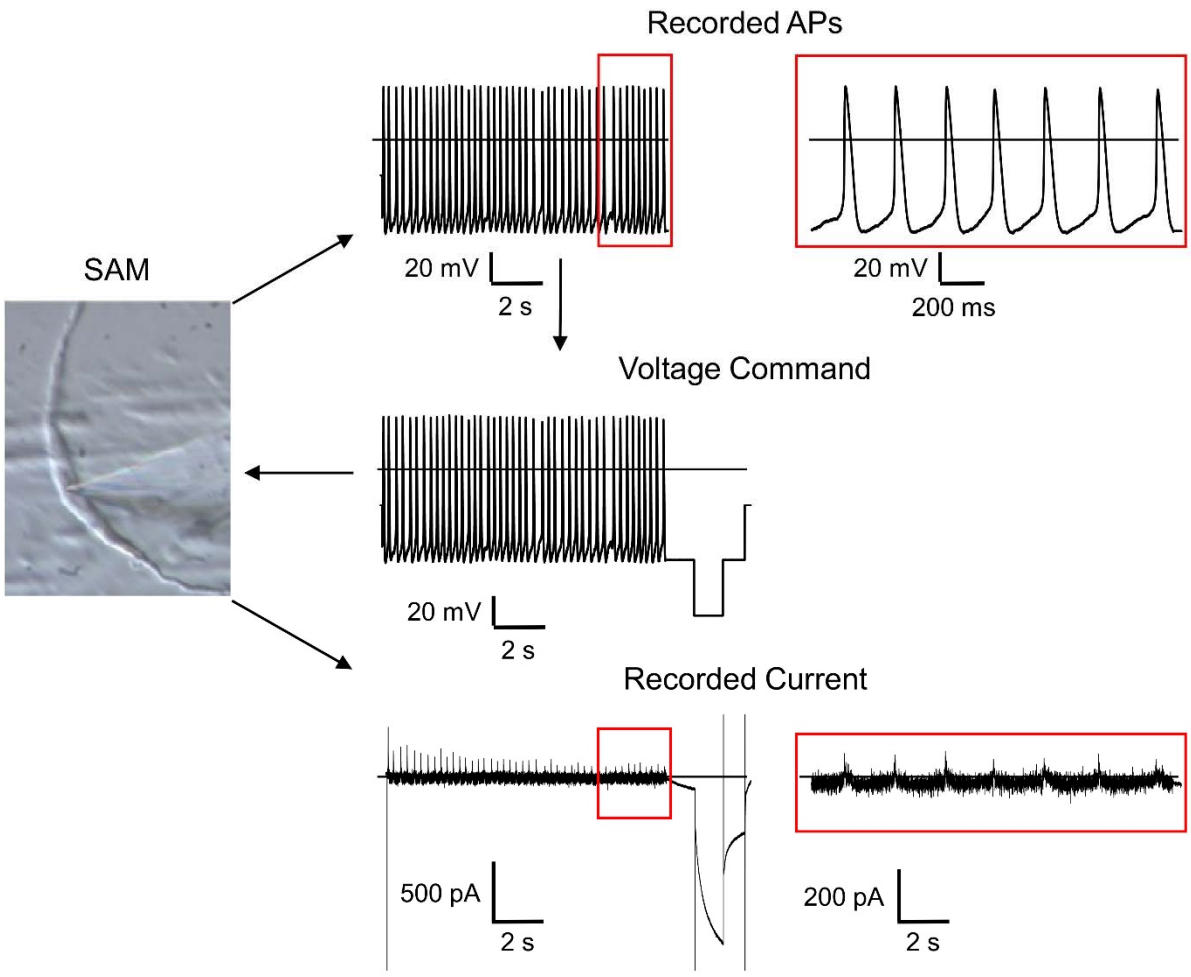

Figure S2: AP clamp methodology

Schematic of the workflow used in AP clamp experiments. Spontaneous APs were first recorded in current clamp mode without injected current (I = 0) from isolated SAMs in either 1 nM or 1 µM isoproterenol (*top* and *top inset*). 10 s of APs were then integrated into a voltage protocol that also included square voltage pulses at the end of each sweep so that drug block could be monitored over time (*middle*). Repeated sweeps of this voltage protocol were then applied to the same myocyte in voltage-clamp mode from a holding potential of -40 mV with an interpulse

interval of 20 s. AP-elicited currents were collected during perfusion of different blocker solutions and were analyzed during the last 2 s of each AP-train, once steady-state current activation had been reached. As expected, the current elicited by APs from the same cell was near zero in the control Tyrode's solution without any drugs (and without whole-cell capacitance compensation) (*bottom* and *bottom inset*). Horizontal lines indicate zero voltage or zero current levels.

Supplementary Figure 3:

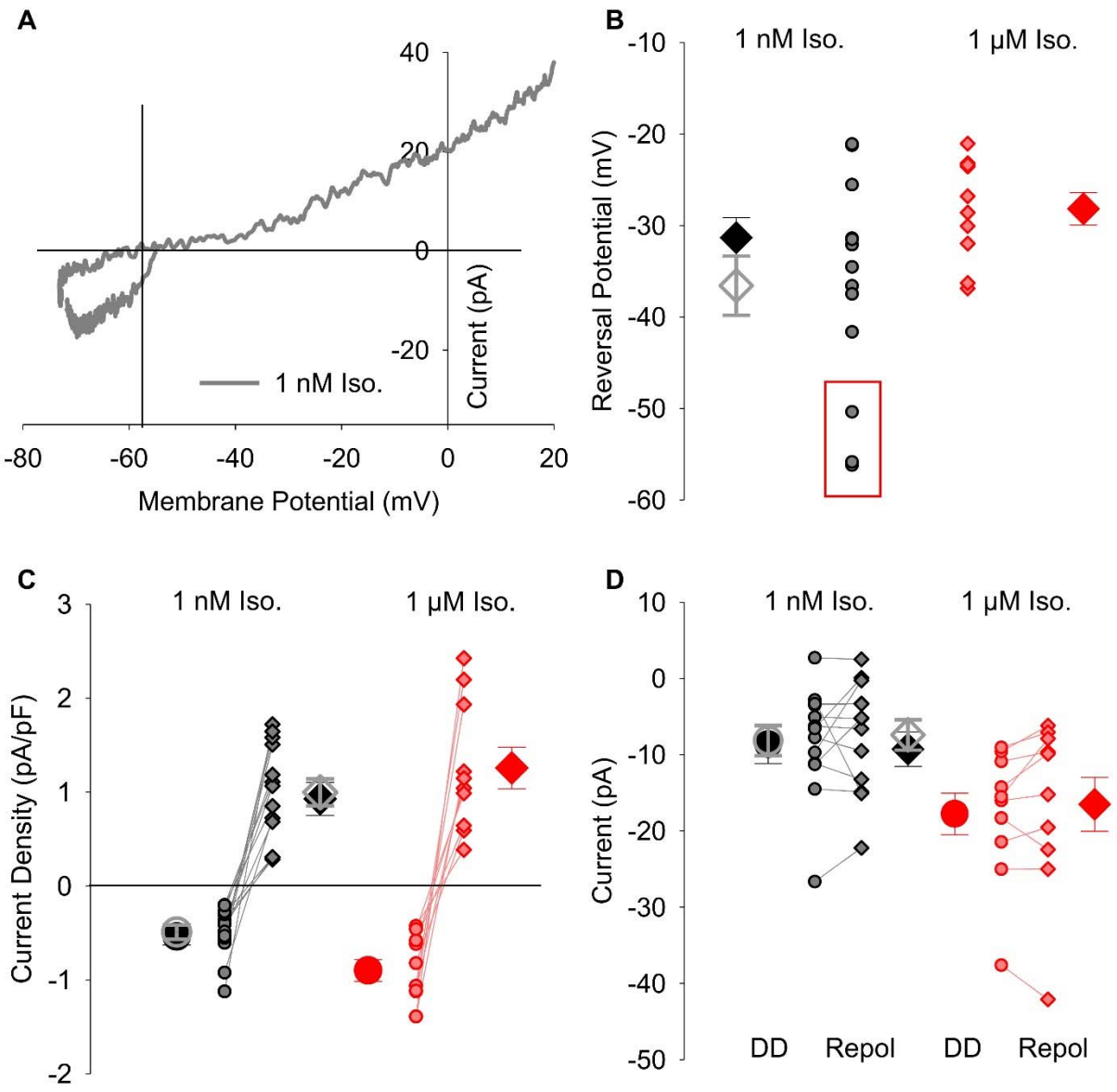

Figure S3: A: Representative ivabradine-sensitive current-voltage relationships from a cell with contamination by an outward K^+ current in 1 nM isoproterenol (*grey*). The reversal potential for this cell was -56 mV (*vertical line*) and the ivabradine-sensitive current displays gating during the diastolic depolarization reflecting deactivation of the K^+ current. **B:** Average (± SEM) reversal potential for ivabradine-sensitive current in 1 nM isoproterenol (*black*), 1 nM

isoproterenol when cells with negative reversal potential are included (*grey*), and 1 μM (*red*) isoproterenol. Individual data points are shown as small symbols. The 3 cells that were not included in the main analysis are indicated by a red box. When these 3 cells are included in the analysis, the reversal potential of I_f differs significantly between 1 nM and 1 μM isoproterenol (unpaired t-test; P = 0.0494). In 1 nM isoproterenol the reversal potential of I_f measured during APs is significantly more hyperpolarized than that measured during hyperpolarizing pulses (Tukey post-hoc test; P = 0.0091) **C:** Average (± SEM) peak inward (*circles*) and outward (*diamonds*) I_f current density in 1 nM isoproterenol, 1 nM isoproterenol with contaminated cells included, and 1 μM isoproterenol using the same colour scheme as **B**. **D:** I_f current amplitude recorded at -60 mV during the diastolic depolarization (DD; *circles*) and following AP repolarization (Repol; *diamonds*) in 1 nM isoproterenol, 1 nM isoproterenol with contaminated cells included, and 1 μM isoproterenol using the same colour scheme as **B**.

Supplementary Figure 4:

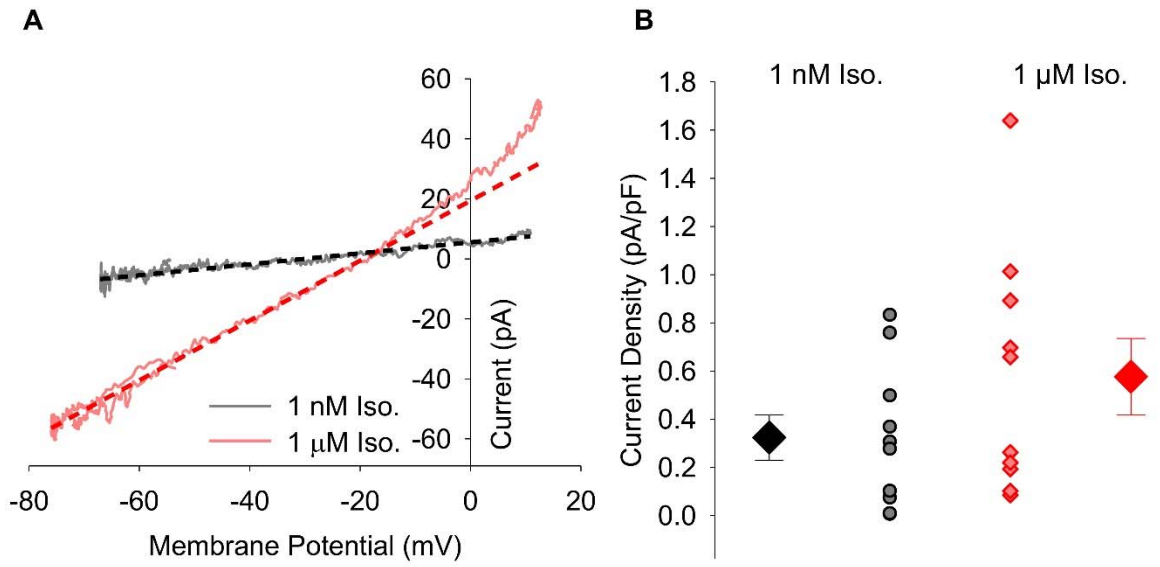

Figure S4: Rectification of the ivabradine-sensitive outward current at depolarized potentials

A: Representative experimental ivabradine-sensitive current-voltage relationships for a single cell in 1 nM isoproterenol (*black*) or 1 µM isoproterenol (*red*) with extrapolated linear fits to data at potentials negative to -20 mV indicated by *dashed lines*. **B:** Average (± SEM) peak outward I_f in SAMs in 1 nM isoproterenol (*black*) or 1 µM isoproterenol (*red*) predicted by extrapolated linear fits to experimental data at potentials below -20 mV. Individual data points are shown as small symbols.

Supplementary Figure 5:

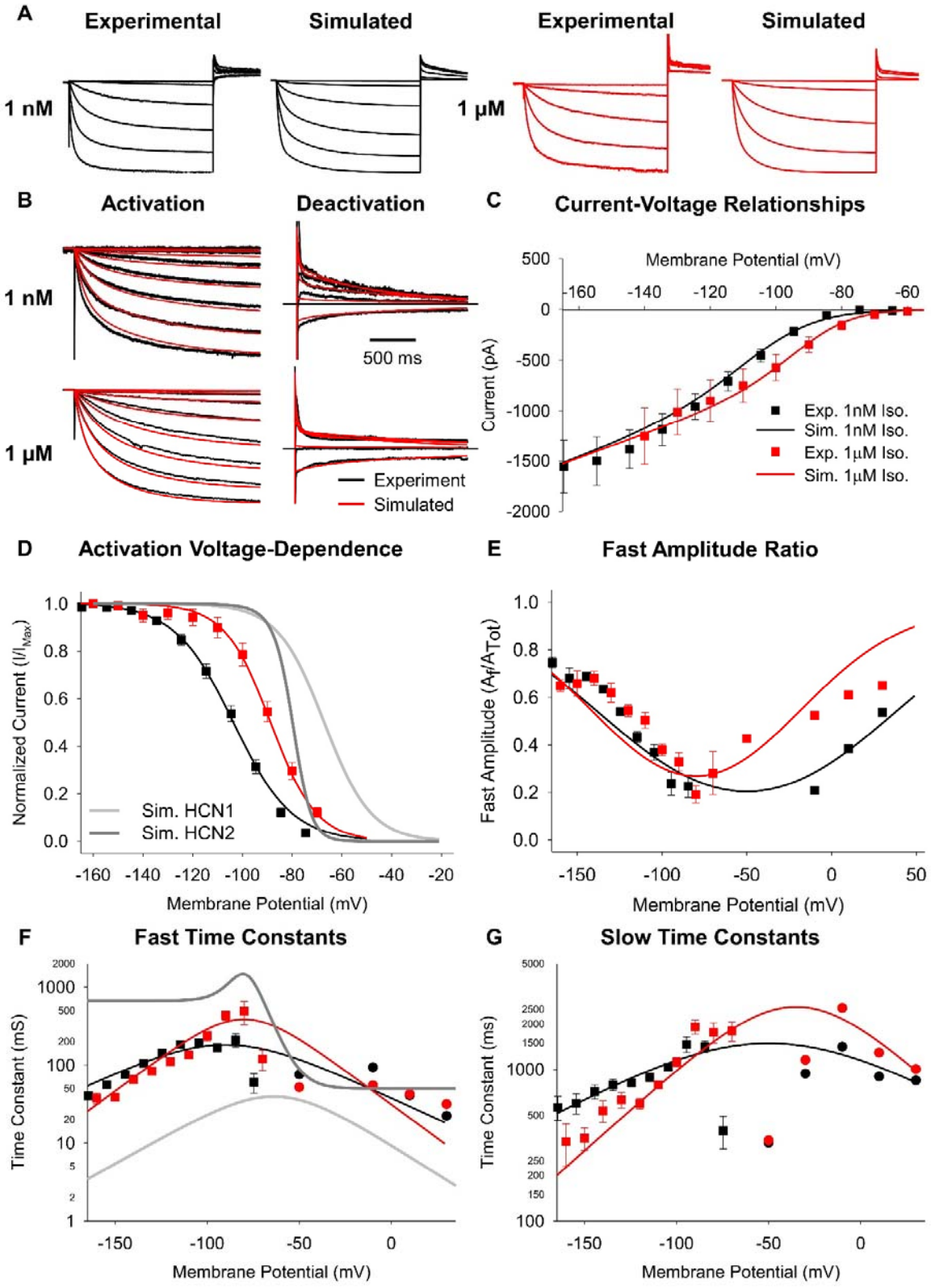

Figure S5: A model of the funny current recapitulates voltage-clamp data from SAMs

A: Experimental and simulated I_f current families in response to 3 s hyperpolarizations to potentials between -50 and -150 mV followed by a depolarizing step to 0 mV in 1 nM (*black*) and 1 μM (*red*) isoproterenol. **B:** Overlaps of experimental (*black*) and simulated (*red*) I_f current activation (*left*) and deactivation (*right*) in 1 nM (*top*) and 1 μM (*bottom*) isoproterenol. **C:** Experimental (*symbols*) and simulated (*lines*) I_f current-voltage relationships in 1 nM (*black*) or 1 μM (*red*) isoproterenol. **D:** Experimental and simulated I_f activation voltage-dependence using the same colour scheme and symbols as **C**. Simulated HCN1 (*light grey*) (5) and HCN2 (*dark grey*) (4) activation voltage-dependence are also plotted. **E:** Experimental and simulated ratios of fast time constant to slow time constant amplitudes using the same colour scheme and symbols as **C**. **F-G:** Experimental and simulated fast (**F**) and slow (**G**) time constants of I_f activation (*squares*) and deactivation (*circles*) using the same colour scheme as **C**. Simulated HCN1 (*light grey*) and HCN2 (*dark grey*) time constants are also plotted in **F**. All experimental values are averages ± SEM. n = 5 to 20.

Supplementary Figure 6:

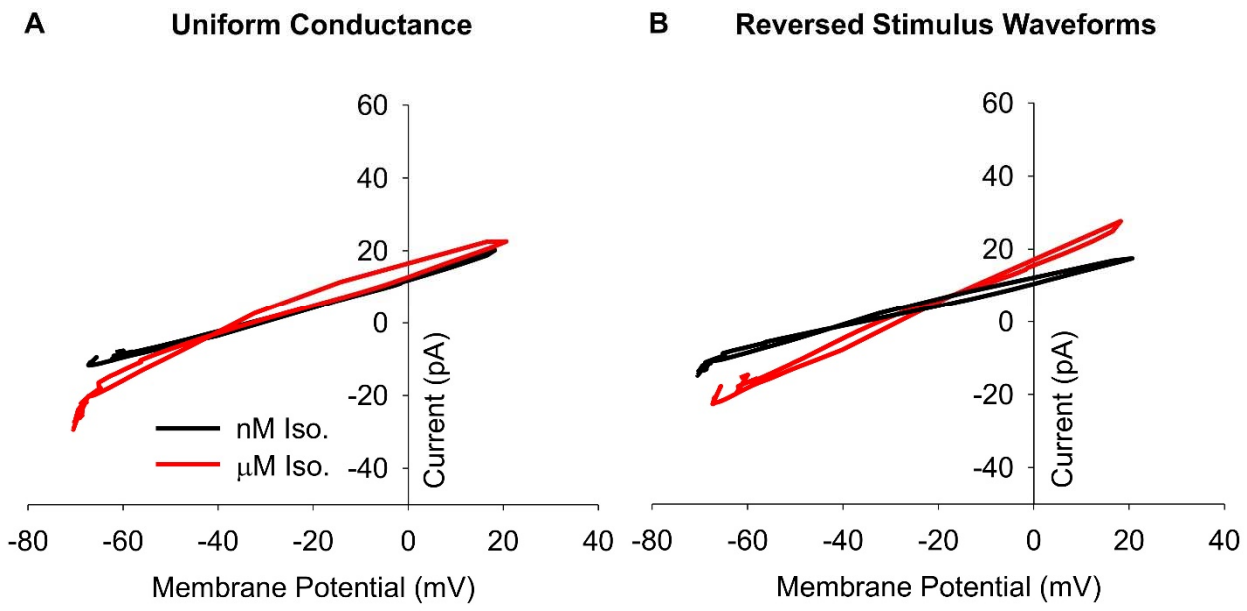

Figure S6: Changes in maximal conductance and AP waveform do not account for differences in the funny current in 1 nM and 1 µM isoproterenol.

A: Average current-voltage relationships of simulated I_f in response to pre-recorded sinoatrial APs simulated using the 1 nM isoproterenol model (*black*) or the 1 µM isoproterenol model (*red*) with the same maximum conductance of 11.79 nS used in all simulations. **B:** Average current-voltage relationships of simulated I_f using the 1 nM isoproterenol model (*black*) simulated with APs recorded in 1 µM isoproterenol or the 1 µM isoproterenol model (*red*) with APs recorded in 1 nM isoproterenol.

Supplementary Figure 7:

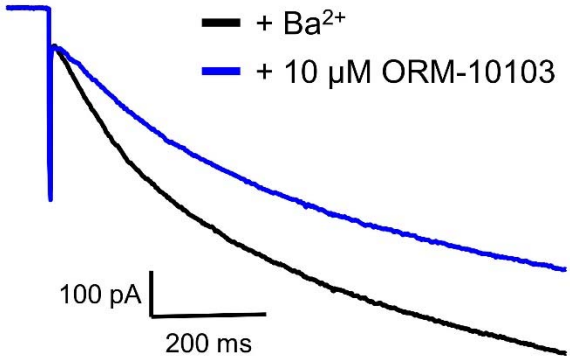

Figure S7: ORM-10103 blocks the funny current in SAMs:

Representative I_f currents recorded at -120 mV in 1 mM $BaCl_2$ in the absence (*black*) or presence of 10 µM ORM-10103. ORM-10103 block the peak inward I_f on average 33 ± 10% (N = 5).

1. Z. Liao, D. Lockhead, E. D. Larson, C. Proenza, Phosphorylation and modulation of hyperpolarization-activated HCN4 channels by protein kinase A in the mouse sinoatrial node. *J. Gen. Physiol.* **136**, 247–258 (2010).

2. Y. Chen-Izu, L. T. Izu, B. Hegyi, T. Bányász, "Recording of Ionic Currents Under Physiological Conditions: Action Potential-Clamp and 'Onion-Peeling' Techniques" in *Modern Tools of Biophysics*, Handbook of Modern Biophysics., T. Jue, Ed. (Springer, 2017), pp. 31–48.

3. S. Kharche, J. Yu, M. Lei, H. Zhang, A mathematical model of action potentials of mouse sinoatrial node cells with molecular bases. *Am. J. Physiol. Heart Circ. Physiol.* **301**, H945-963 (2011).

4. J. Wang, S. Chen, M. F. Nolan, S. A. Siegelbaum, Activity-Dependent Regulation of HCN Pacemaker Channels by Cyclic AMP: Signaling through Dynamic Allosteric Coupling. *Neuron* **36**, 451–461 (2002).

5. A. Battefeld, N. Rocha, K. Stadler, A. U. Bräuer, U. Strauss, Distinct perinatal features of the hyperpolarization-activated non-selective cation current Ih in the rat cortical plate. *Neural Develop.* **7**, 21 (2012).